Cumulative method of image reconstruction in synthetic aperture - theory and experimental results

J. Wójcik, I. Trots, A. Nowicki, M. Lewandowski
Department of Ultrasound
Institute of Fundamental Technological Research PAS
Warsaw, Poland
jwojcik@ippt.pan.pl

Abstract—**The Synthetic Aperture (SA) method provides a new solution in ultrasound diagnostics. It has particular importance in applications where frame rate and image resolution are crucial. Our new approach named Cumulative Synthetic Transmit Aperture (CSTA) allows optimizing SA in terms of memory size and computational power. The proposed CSTA algorithm requires 25 times less memory than a reference STA method for 64 elements transducer. This makes feasible implementation of CSTA on a low-power embedded GPU.**

Keywords— ultrasonic imaging; synthetic aperture; GPU

I. INTRODUCTION

The Synthetic Aperture (SA) method provides a new solution in ultrasound diagnostics and has particular importance in applications where frame rate and image resolution are crucial. Our new approach, named Cumulative Synthetic Transmit Aperture (CSTA), allows optimizing SA in terms of the memory size and computational power. With the advent of GPU (graphics processor unit) processing era a real-time SA processing became feasible. However, a required memory transfer starts to be a limiting factor. The proposed CSTA algorithm requires 25 times less memory than a reference STA method for 64 elements transducer. This makes feasible a low-power implementation of CSTA on embedded GPU.

The application of synthetic aperture is a radical change when compared to currently used scanners where image are created line by line. So far in ultrasonography the way of image formation considerably limits resolution, acquisition speed as well as possibility of obtaining sufficient imaging data of high quality. The synthetic aperture method solves these problems by using wide spatial spectrum of constituent elements that allows to obtain data in a wide angular range simultaneously in a few transmissions [1].

A performance optimization of the SA implementation consists in finding an optimal relation between memory required for acquisition of the ultrasound echoes, reconstruction time and computational power necessary for reconstructing the image.

Our goal is to reduce memory and computational requirements of the SA method while maintaining an acceptable image quality when compared to the known or applied methods.

II. METHODS

A. Physical model

In theoretical development of the CSTA algorithm the Rayleigh-Sommerfeld solutions to a boundary-value problem of Dirichlet for the Helmholtz equation were used. The distinctive feature of the CSTA is accumulating of echoes of subsequent transmissions in only one matrix, which is sufficient for data acquisition and image synthesis. In traditionally applied STA separate acquisition matrices for each transmission are created. Next, for each acquisition only fragments of the images are reconstructed from the subsequent matrices.

The proposed physical model describing acoustic field generation, its propagation in a heterogeneous medium (scattering) and detection, is based on Sturm-Liouville (SL) equation (modified Helmholtz equation) [2].

For the modeling purpose it is assumed that scattering occurs on the point heterogeneity with elementary target strength which can take any coordinate $\mathbf{R} \equiv [z, \mathbf{r}], \mathbf{r} \equiv [x, y]$ in the imaging area. Then scattering potential in SL equation is replaced by $V(\mathbf{R}') = v\delta(\mathbf{R}'-\mathbf{R})$, $v = const$, where $\delta(\bullet)$ is the Dirac distribution, v is the "target strength" of a point scatterer. The L element linear array of identical elementary transmit-receive transducers is modeled by rectangular apertures located with pitch D on the plane z=0 (Fig. 1).

The above assumptions are sufficient for basic, correct analysis of transmit/receive characteristics of transducers and their combinations which are important for this work. They are also used in literature [3].

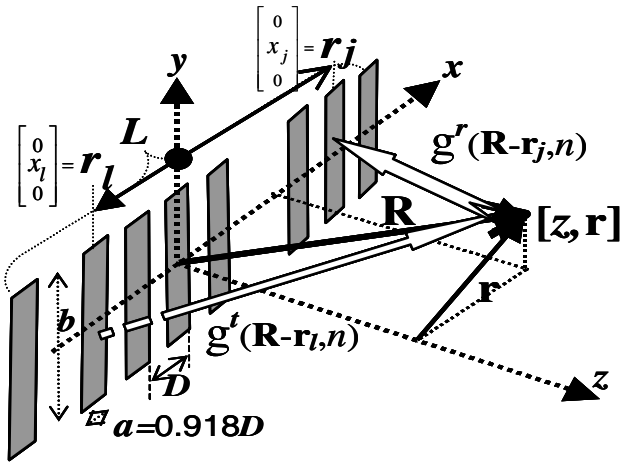

Figure 1. The linear array of transducers modeled by rectangular apertures.

The spectrum of the field scattered in **R**, received by *j*-th transducer and registered in *j*-th channel after *m*- th burst is given by:

$$E(\mathbf{R},n,j;m) \equiv vc^{rt}(n) q_{r_j}^{m} g^{r}(\mathbf{R}-\mathbf{r}_j,n) \cdot \cdot \sum_{l} q_{t_l}^{m} g^{t}(\mathbf{R}-\mathbf{r}_l,n), \quad m=1,\ldots,M \tag{1}$$

Where the transmit g^t and receive g^r characteristics are the solutions of Helmotz equation according to Dirichlet and Neumann boundary value problems for z=0 and in the half space $z \geq 0$; $q_{t_l}^{m}$, $q_{r_l}^{m}$ are the L element pairs of sequences (**..,0,...,1,..**) determining elements active (,**1,**), in transmitting and in receiving; $c^{rt} \equiv c^r c^t$, $c^r(n)$ is the receiver frequency response, $c^t(n)$ is the transmitted impulse spectrum; $r_l \equiv [0, x_l, 0]$ is the *l*-th transducer position; *M* - number of transmissions.

The echo from the scatterer in $\mathbf{R}=\mathbf{R}_c$ registered in *j*-th channel after *m*-th burst (in *m*-th acquisition matrix) has the following form:

$$P(t,\mathbf{R}_c,j;m) = F^{-1}[E;t] = P(t-\tau^m(\mathbf{R}_c,j)), \tag{2}$$

where: t is the time (or discrete time t_v); $\tau^m(\mathbf{R}_c,j) \equiv |\mathbf{R}_c - \mathbf{r}_j| + d(\mathbf{R}_c,m)$, $d(\mathbf{R}_c;m)$ is effective (wave) range of the transmitting sequence $q_{t_l}^{m}$ (active elements) from point $\mathbf{R}_c$. Only for few/not numerous classes of SA $d(\ ,j;m)$ has a simple function of practical significance. In a dynamic focusing method the image (Pi(•)) is obtained as a result of adding up the fragments of the wave form recorded in the receive channels with the simultaneous compensation of their phases $\tau^m(\mathbf{R}_c,j)$. From the m-th acquisition matrix it is obtained:

$$\mathrm{Pi}(\mathbf{R},\mathbf{R}_c;m) = \sum_{j}^{L} P(\tau^m(\mathbf{R},j) - \tau^m(\mathbf{R}_c,j),j;m). \tag{3}$$

Generally, the result image of the object is obtained by combining the images from all *M* bursts:

$$\mathrm{Pi}(\mathbf{R},\mathbf{R}_c) = \sum_{m=1}^{M} \chi(\mathbf{R};m)\,\mathrm{Pi}(\mathbf{R},\mathbf{R}_c;m). \tag{4}$$

The coefficients χ can be complex functions. In the STA presented below, χ are masking functions, formally defining a part of the entire imaged field which appears as a result of the *m*-th burst (from the *m*-th acquisition matrix)

$$\chi(\mathbf{R},m) \equiv rect\left((x-xt_m)/\Delta x; 0<z\leq z_{\max}, y=0\right), \tag{5}$$

xt_m are the centers of the active parts of transmitting sequences. It is assumed that $|xt_m - xt_{m-1}| = 2\Delta x (=2D)$ It means that the entire image is a sum of *M* not overlapping partial images created from the *M* acquisition matrix.

In the presented CSTA all $\chi(\mathbf{R},m) \equiv 1$. In this case adding images can be substituted by adding the echoes Eq. 2. After each *m*-th burst the echoes (or spectra) are added in each of *j* channels to the echoes existing after the *m-1*-th burst. This way instead of *M* acquisition matrices we have only one which is used to create an image.

$$\mathrm{Pi}(\mathbf{R},\mathbf{R}_c) = \sum_{j}^{L} \mathrm{P}\left(\tau(\mathbf{R},j) - \tau(\mathbf{R}_c,j), j\right) \tag{6}$$

$$\mathrm{P}(t-\tau(\mathbf{R}_c,j),j) \equiv \sum_{m}^{M} P\left(t-\tau^m(\mathbf{R}_c,j),j;m\right)$$

where: $\tau(R_{(c)},j) \equiv |\mathbf{R}_{(c)} - \mathbf{r}_j| + d(\mathbf{R}_{(c)})$. The complex spectral analysis of Eq. 1 gives exact form of $d(\cdot)$ it weakly depends on b (Figure 1). Nevertheless in good approximation $d(\mathbf{R},b) \cong z$. For STA $d(\mathbf{R};m) = \sqrt{(x-xt_m)^2 + z^2}$ is applied.

B. Numerical and Experimental Setup

In the conducted numerical and experimental study in both methods for every *m* (bursts) receiving sequences with the maximum number of active in reception transducers *Lr*=*L*(=64) $q_{r_j}^{m} = 1$ were used for all j. The pattern of transmitting sequences are defined as follows

$$qt_l^m \equiv \begin{cases} 1 \ for \ 1 \leq l_m + 1 \leq l \leq l_m + Lt \leq L \\ 0 \quad for \ other \ \ l \end{cases}, \tag{7}$$

where $l_m \equiv (m-1)\cdot sh$, $m = 1,2,\ldots,M \equiv 1 + (L-Lt)/sh$, and are identical for both methods (Figure 2).

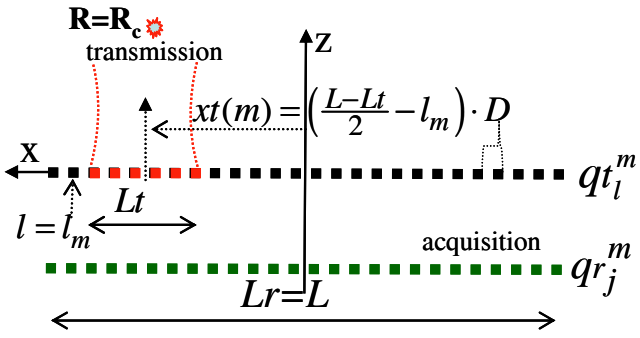

Figure 2. Diagram of transmitting and receiving sequence for certain m, $xt(m)=xt_m$.

The diagrams in Figure 3 illustrate the subsequent m-sequences of the transmission, respective acquisition sequences and acquisition matrices as well as characteristic way of image creation.

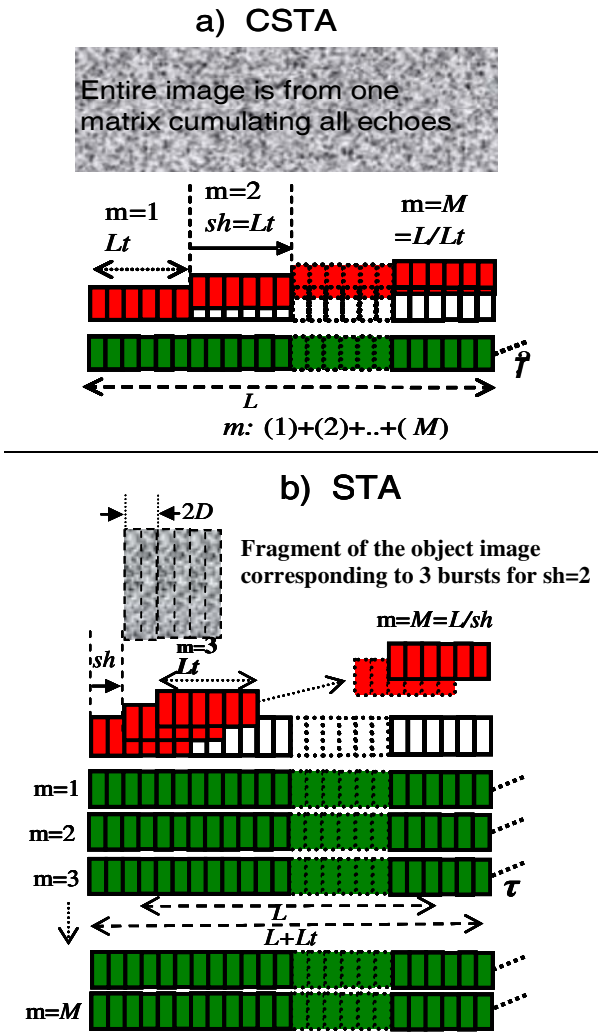

Figure 3. Diagrams of transmission, acquisition and imaging in: a) CSTA, b) STA.
Transmitting sequences are red, receiving transducers and acquisition matrices – green.

The characteristic feature of CSTA is that independently on the number of transmissions M all echoes are collected in one $Lx\tau$ matrix (τ - the number of echo samples in each of channels). From the echo samples which are collected in this matrix according to formula (6) the entire image of the object is created at least L lines in width. The information about the position of transmitting sequence xt(m) is not needed to calculate time delays from the transmitting sequence to the scatterers. In the simplest version the sequence of Lt transducers transmits simultaneously. It is assumed that such natural M number, the number of transmissions bursts, is chosen that $L = M \cdot Lt$. After each m burst the echo samples are recorded in the described above matrix and added to the existing after the previous m-1-th burst the transmitting sequence is shifted by $sh=Lt$ transducers (Figure 3a). In other SA cases the echo acquisition in separate for every burst matrix is applied. Namely, if we want to create the L-line wide image ($L \cdot D$ mm) transmitted by Lt transducers (transmitting sequences have to be $L+Lt$ long), than after each m-th burst the m-th acquisition matrix is created and the transmitting sequence is shifted by sh lines ($sh \cdot D$ mm). The entire image is created from $M=(L/sh)$ partial images according to the formula (4), each sh lines in width ($sh \cdot D$ mm) is corresponding to center lines of transmitting sequences. The memory and time needed for image reconstruction are characterized by numbers Mem ~$(L+Lt)(L/sh)$, Time~$M=(L/sh)$. In the discussed CSTA case Mem~L and Time~$M=L/Lt$, respectively.

III. Results

For both STA and CSTA methods the L=64 elements of linear array was synthesized. The receiving sequence Lr, for both STA and CSTA, was equal to full aperture of 64 elements. The transmitting groups were also the same and equal to 16. For CSTA the scanning step was equal to the number of transmitting transducers (16), what means that for one acquisition matrix four transmission were executed. For standard STA the scanning step was equal to 2 elements, 25 transmissions, and 25 acquisition matrices were built up. Experimental data from a tissue phantom were obtained with the Ultrasonix SonixTouch (Canada) research scanner and specially crafted scripts.

The comparison of reconstructed 2D images using both methods on the wire and tissue mimicking phantoms, as well as their cross-sections in linear and logarithmic scales are presented (Figure 4, 5, 6). No special methods of improving image quality were used. The signal controlling the brightness of imaged pixels is $\left|\mathrm{Pi}(\mathbf{R},\mathbf{R}_c)\right|$ for formula (6) - CSTA and (4) - STA. Images width are: $80D$=**24mm** for CSTA and $M \bullet sh$ $=50D$=**15mm** for STA.

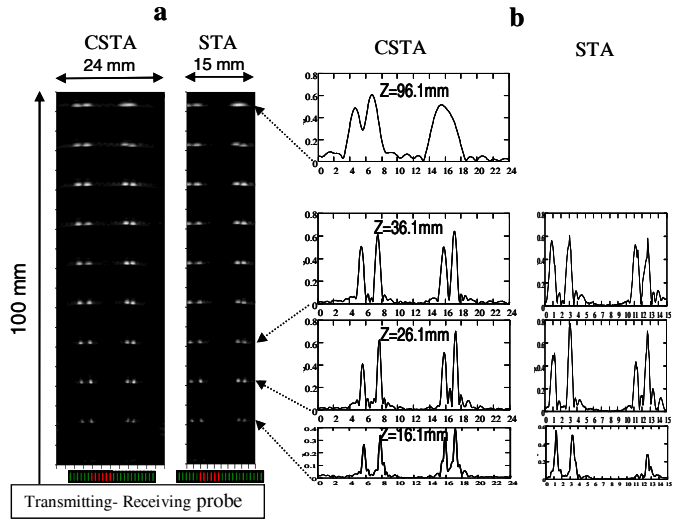

Figure 4. Images of wire phantom immersed in water in linear grayscale (a). Cross-section at marked by arrows depths z (b).

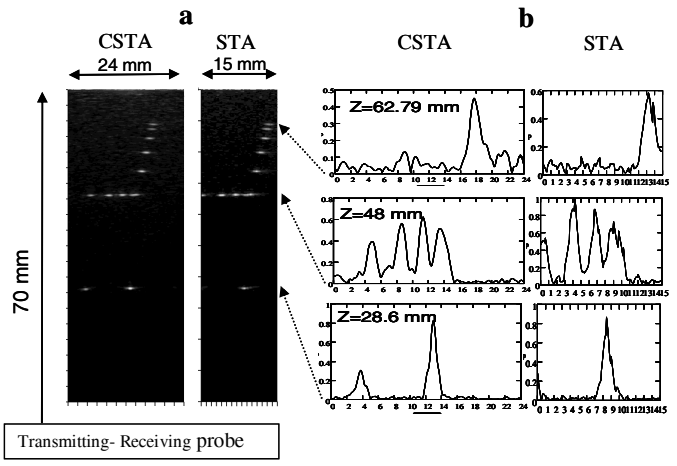

Figure 5. Images of tissue mimicking phantom in water in linear grayscale (a) and the cross-section at depths z (b).

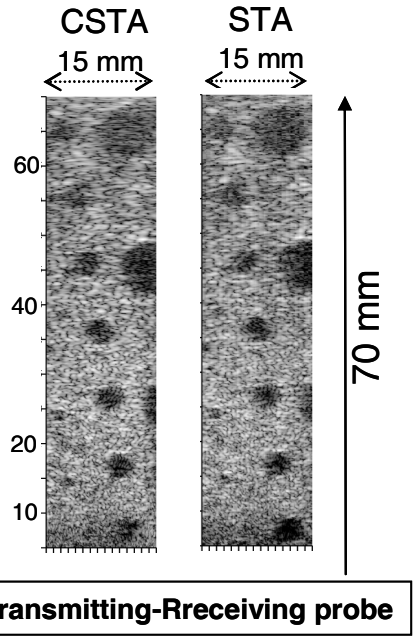

Figure 6. Images of tissue mimicking phantom with cysts in logarithmic grayscale.

IV. CONCLUSIONS

The obtained CSTA images clearly show comparable resolution and contrast to the reference STA, while the memory/processing cost is at 25 times lower. This reduction makes feasible real-time implementation of CSTA imaging on a low-power embedded GPU. Moreover, it can be easily expended to higher Lr=2,3 (CSTA) R-Receive.

ACKNOWLEDGMENT

Research co-financed by the Ministry of Science and Higher Education, Poland (Grant No. N518-503339) and by the European Regional Development Fund under the Innovative Economy Operational Programme (Project POIG.01.03.01-14-012/08-00).

REFERENCES

[1] I. Trots, A. Nowicki, M. Lewandowski; Synthetic transmit aperture in ultrasound imaging. Archives of Acoustics, 43(4):685–695, 2009.

[2] J. Wojcik, J. Litniewski, A. Nowicki; Modeling and analysis of multiple scattering of acoustic waves in complex media: Application to the trabecular bone. J. Acoust. Soc. Am. 130(4):1908-1918, 2011.

[3] J.A. Jensen, Linear description of ultrasound imaging systems; Notes for the International Summer School on Advanced Ultrasound Imaging, Technical University of Denmark, 1999